

Grooving the carbon nanotube oscillators

Lai-Ho Wong, Yang Zhao,^{a)} and GuanHua Chen
Department of Chemistry, University of Hong Kong, Hong Kong, People's Republic of China

Allen T. Chwang
Department of Mechanical Engineering, University of Hong Kong, Hong Kong, People's Republic of China

(Received 17 November 2005; accepted 14 March 2006; published online 3 May 2006)

Using microcanonical molecular dynamics, we investigate effects of single defects on the performance of a nanoscale oscillator composed of coaxial double-walled carbon nanotubes. It is found that at low temperatures a single defect placed on the outer nanotube can significantly reduce axial oscillation energy leakage by impeding intertube rotational modes, and therefore mitigates the frictional effects between sliding nanotubes. © 2006 American Institute of Physics.

[DOI: [10.1063/1.2199471](https://doi.org/10.1063/1.2199471)]

Synthesis of large quantities of carbon nanotubes^{1,2} (CNTs) has recently been made possible by carbon-arc vaporization and transition-metal catalytic reaction techniques. The latter method has been used to synthesize single wall nanotubes (SWNTs).^{3,4} A CNT is a rolled-up graphite sheet labeled by its chiral vector (m, n) .^{5,6} A sundry variety of applications have been found for CNTs, including single-electron transistors,⁷ tunnelling-magnetoresistance devices,⁸ CNT diodes,⁹ intramolecular junctions,¹⁰ molecular bearings,^{11,12} springs,¹³ hooks,¹⁴ and oscillators.^{15–19} Evidently, there emerges a promising field of nanoelectromechanical systems²⁰ (NEMS) that utilize carbon nanotubes as the basic building blocks.

The friction phenomenon, or the energy dissipation between two contacting parties which slide with respect to each other, is in general taken to denote the conversion of orderly translational energies into disorderly vibrational energies. The traditional understanding of the friction phenomenon fails to apply to nanoscale machinery. Consequently, performance, friction, stabilities, and load-bearing properties of nanobearings, nanosprings, nano-oscillators, and other fundamental components of these nanomachines await systematic explorations via both theoretical and experimental means. In the traditional mechanical oscillators, grooves along the direction of oscillation often reduce motion instabilities, and therefore, mitigate unwanted frictional effects. For nanoscopic devices, an intriguing question would be whether such grooves can still be devised and put to use to ensure smooth performance of the nano-oscillators while suppressing its undesired energetic rivals. In an earlier study on double-walled carbon nanotube (DWNT) oscillators,²¹ it has been found that one significant channel for energies in the axial motion to leak into the pool of disorderly phonons is through intertube rotation, and that rocking motion of the inner tube and wavy motion of the outer tube also play a significant role in the energy dissipation process. To remedy energy leaks via intertube rotation, an atomic-scale grooving on the DWNT oscillator is devised by simply embedding a single defect in the outer nanotube.

This work is aimed to establish an understanding of atomic-scale grooving in nano-oscillators. Point defects on

the outer nanotube will be examined, and proposals on atomic-scale grooving will be made to improve mechanical performance of DWNT oscillators. Properly introducing single or line defects, namely, the atomic-scale grooves, may force the oscillating core to stay in-line with its housing and thus prevent intertube rotational movements, and in this case, the defects act much like the grooves in the conventional mechanical oscillators that stabilize the translational motion. We expect that our findings here to have significant implications to developing not only the CNT-based gigahertz oscillators but also NEMS devices in general with components moving in the gigahertz range.

Motivated by dynamic and static friction measurements by Cumings and Zettl¹³ and by Yu *et al.*²² we have previously conducted tribological studies for systems of concentric carbon nanotube systems, one of the most elementary realizations of such an oscillator, using molecular dynamics (MD) in a microcanonical ensemble.¹⁶ DWNT oscillators of various lengths and constructions are compared for their oscillation resilience under motion-induced self-heating. We have shown that frictional behavior in these oscillators in a microcanonical ensemble can be associated primarily with off-axial rocking motion of the inner nanotube and wavy motion of the outer nanotube, which may or may not occur, depending upon both the configurations of individual oscillators and the initial system energies, and that the oscillation is nearly frictionless in the absence of the rocking and wavy motions. Furthermore, the friction phenomenon in nano-oscillators represents a more general problem of transfer of energies from the orderly degrees of freedom in a nanostructure into disorderly phonons. The collective motion that underlies nanoscale friction may manifest itself in other forms under various other circumstances (such as nanosprings¹¹), but the fact remains that the energy transfer channels are facilitated by collective modes in the nanosystems in the process of moving energies into disorderly phonons.

The DWNT oscillator studied here have (9,0) and (18,0) nanotubes as the inner and outer tubes, respectively. The inner nanotube is 25.4 Å in length, and the outer one, 37 Å. The intertube distance is ~3.4 Å, which coincides that between adjacent sheets of graphite. The simplest atomic-scale groove on the DWNT oscillator comprises of a single defect in the outer nanotube, as displayed in Fig. 1. A defect in a

^{a)}Electronic mail: yang@yangtze.hku.hk

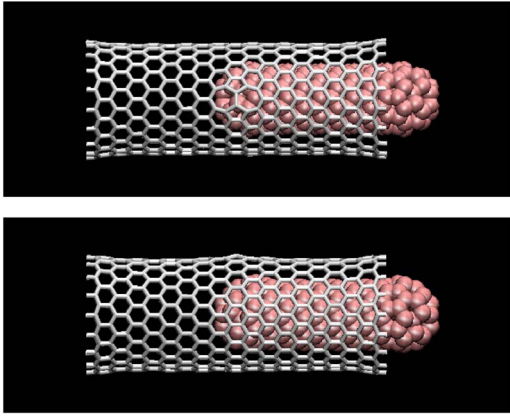


FIG. 1. Double-walled carbon nanotube oscillator with a single defect in the outer nanotube. Upper panel: top view; lower panel: side view.

carbon nanotube is regarded as nonhexagonal ring structures embedded in the carbon nanotube hexagonal network. The optimum bond angle for sp^2 hybridized carbon is about 120° , a nonhexagonal ring structure is therefore subject to higher angle strain. To fulfill the topological requirement and avoid high angle strain, the single defect introduced in the outer sheath is made of two sets of pentagon-heptagon pairs as shown in the upper panel of Fig. 1.

Prior to simulation, the DWNT oscillator is connected to a thermostat and heated up to an initial temperature T_i , and sufficient time is given for it to equilibrate thermally. At the beginning of simulation, $t=0$, the inner tube is pulled out of the outer tube along their common axis, and the system is detached from the thermostat. A portion of the inner tube is thus exposed, the length of which at the beginning of the simulation is defined as the initial extrusion length s . The inner tube is then released with zero initial speed. The CHARMM force field is being used for both geometry optimization and molecular dynamics simulation. The former is performed with the method of steepest descent. A time step of 1 fs is used in the MD simulation. Instead of monitoring the system potential energy or the oscillation amplitude,^{17,18} we focus on the phonon kinetic energies, i.e., the relative kinetic energy of two nanotubes defined as

$$K_{\text{rel}}(t) \equiv \sum_i \frac{1}{2} m_i |\mathbf{v}_i^{\text{in}} - \mathbf{v}_{\text{ave}}^{\text{in}}|^2 + \sum_j \frac{1}{2} m_j |\mathbf{v}_j^{\text{out}} - \mathbf{v}_{\text{ave}}^{\text{out}}|^2, \quad (1)$$

where \mathbf{v}_i^{in} ($\mathbf{v}_j^{\text{out}}$) and m_i (m_j) are the velocity and the mass of the i th (j th) atom in the inner (outer) tube, respectively; $\mathbf{v}_{\text{ave}}^{\text{in}}$ ($\mathbf{v}_{\text{ave}}^{\text{out}}$) is the average atomic speed of the inner (outer) tube. $K_{\text{rel}}(t)$ is a direct measure of the intratube temperature, i.e., an indicator of heat transfer from the orderly translational motion. For low-energy oscillations in which the intratube motion of the carbon atoms is mostly harmonic with energies equally distributed into kinetic and potential portions, Eq. (1) is approximately one-half of $E_{\text{loss}}(t)$, the combined loss of intertube potential energy and the orderly translational kinetic energy,

$$E_{\text{loss}}(t) \equiv E_{\text{tot}}(0) - [P_{\text{trans}}(t) + K_{\text{trans}}(t)], \quad (2)$$

where $E_{\text{tot}}(0)$ is the initial total system energy at $t=0$, $P_{\text{trans}}(t)$ is the time-dependent potential energy between two nanotubes due to translational oscillation (while freezing the atoms in both nanotubes), and $K_{\text{trans}}(t)$ is the corresponding translational kinetic energy. $E_{\text{tot}}(0)$ is in fact the initial excess

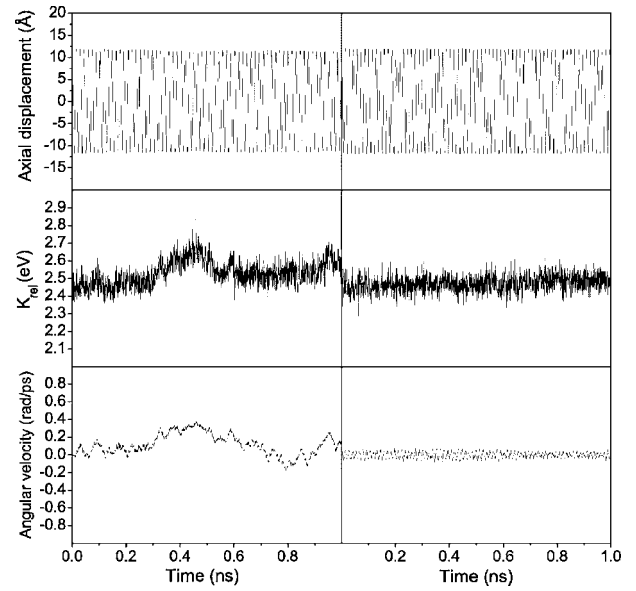


FIG. 2. Comparison between DWNT oscillators with (right column) and without (left column) a single defect. Initial extrusion length $s=6.2 \text{ \AA}$, and the preoscillation temperature $T_i=20 \text{ K}$. Upper two panels: the center-of-mass distance between two nanotubes as a function of time; middle two panels: the relative kinetic energy as a function of time; lower two panels: the intertube angular velocity between the two nanotubes as a function of time.

intertube van der Waals energy, which is set to zero if both nanotubes sharing a common axis are kept still.

In Fig. 2 we compare dynamics of DWNT oscillators with and without a single defect. Initial extrusion length $s=6.2 \text{ \AA}$, and the presimulation temperature $T_i=20 \text{ K}$. The center-of-mass distance between two nanotubes as a function of time is displayed in upper two panels. Contrary to our expectation, the oscillator with the single defect in its outer nanotube (right panel) retains its initial oscillation amplitude better than the one without defects (left panel). This is confirmed by the relative kinetic energy $K_{\text{rel}}(t)$ as a function of time plotted in the middle panels of Fig. 2. As an indicator for the intratube temperature, $K_{\text{rel}}(t)$ is slightly larger for the oscillator without defects revealing more energetic loss for the axial intertube oscillation and therefore more friction in the DWNT oscillator without defects. Further proof is presented in the lower panels where relative intertube angular velocities are plotted as a function of time. In the absence of defects, the DWNT oscillator sees a significant amount of axial oscillational energies channelled into and out of the intertube rotational modes aiding the frictional effect. For the oscillator modified with a single defect, the relative angular velocity has a restrained amplitude throughout leading to significantly reduced friction between two nanotubes. Corresponding calculations for higher presimulation temperatures, such as $T_i=100 \text{ K}$, have also been conducted, and results show that an increased degree of thermal agitation leads to greater frictional effects for both types of oscillators, and that the ability of single defects to mitigate intertube rotation decreases with increasing presimulation temperature. Frictional forces per atom have been estimated for oscillators with and without defects. For $T_i=20 \text{ K}$, frictional forces for the perfect oscillator and the modified oscillator are estimated to be 7×10^{-16} and $1 \times 10^{-16} \text{ N/at.}$, respectively. As expected, the single defect in the modified system significantly reduces the intertube friction during axial oscillation.

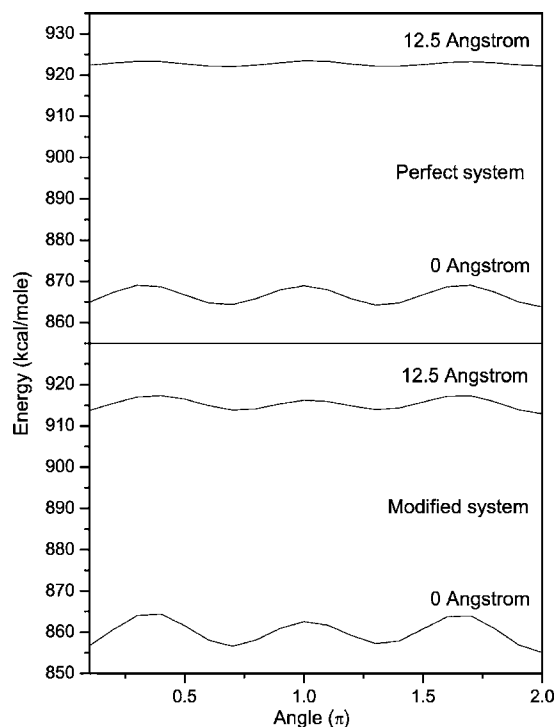


FIG. 3. Comparison of the potential energy as a function of the relative intertube angle between DWNT oscillators with (lower panel) and without (upper panel) a single defect. Two center-of-mass distances are shown: 0 Å (bottom curves in the two panels) and 12.5 Å (upper curves in the two panels).

In Fig. 3 the van der Waals potential energy is plotted as a function of the relative intertube angle for both the defect-free oscillator (upper panel) and the modified oscillator (lower panel). There is threefold symmetry in the potential energy with respect to the relative intertube rotation, which has its origin in the half-fullerene caps of the inner nanotube. For the defect-free oscillator, the depth of the angular potential wells drops drastically when one end of the inner nanotube is extruded out of the outer sheath. As a result, the potential curve is rather flat when the inner tube is displaced by 12.5 Å. For the modified oscillator, however, the depth of the angular potential wells decreases much slower as the inner nanotube is extruded. When the inner tube displacement reaches 12.5 Å, a significant potential depth is retained as shown in the lower panel of Fig. 3.

Rotational energy barriers in defect-free DWNT oscillators originate in the lack of circular symmetry in interactions between inner tube end caps and the outer sheath. When the inner tube is extruded, one end of the inner tube is less rotationally hindered by the outer tube, the angular potential wells flatten spanning intertube rotation upon small perturbations. However, for modified oscillators, the outer nanotube does not possess circular symmetry due to the introduction of the single defect, and as a result, the angular potential barrier persists when the inner tube is extruded. The single defect therefore acts as a groove that prevents intertube rotation from taking place in the DWNT axial oscillator.

Tangential forces on the inner nanotube against intertube rotation can be inferred from potential profiles in Fig. 3. In the defect-free oscillator, maximum tangential forces are estimated to be 5.7×10^{-13} N/at. before extrusion, and 2×10^{-13} N/at. after the intertube displacement reaches

12.5 Å. For the modified system, however, maximum tangential forces are found to be 9.4×10^{-13} N/at. before extrusion, and 5.6×10^{-13} N/at. after the intertube displacement reaches 12.5 Å. The single defect in the modified system thus provides extrusion-insensitive barriers against intertube rotation. As a comparison, restoring forces for the oscillators, which maximize at the positions of maximum extrusions, vary from 10^{-12} to 10^{-11} N/at. while axial frictional forces are estimated to vary from 10^{-16} to 10^{-15} N/at., depending on the presimulation temperature and whether the oscillator contains single defects. Our simulation also reveals that the higher the presimulation temperature, the larger the intertube friction, and the less effective the grooving effect of the single defect in the outer sheath of the DWNT oscillator. Addition of multiple defects is expected to have similar constraining effects for the DWNT oscillator, however, with the increase of the defect number, axial motion stability may become problematic, and additional defect-induced dissipation mechanisms can come into play and raise the DWNT temperature to an operationally undesirable range. Related work has been reported in Ref. 23.

Support from the Hong Kong Research Grants Council (HKU 7012/04P and HKU 7056/01E) and the Committee on Research and Conference Grants (CRCG) of University of Hong Kong is gratefully acknowledged.

- ¹S. Iijima, *Nature (London)* **354**, 56 (1991).
- ²T. W. Ebbesen and P. M. Ajayan, *Nature (London)* **358**, 220 (1992); T. W. Ebbesen, H. Hiura, J. Fujita, Y. Ochiai, S. Matsui, and K. Tanigaki, *Chem. Phys. Lett.* **209**, 83 (1993).
- ³S. Iijima and T. Ichihashi, *Nature (London)* **363**, 603 (1993).
- ⁴D. S. Bethune, C. H. Klang, M. S. De Vries, G. Gorman, R. Savoy, J. Vazquez, and R. Beyers, *Nature (London)* **363**, 605 (1993).
- ⁵C. T. White, D. H. Robertson, and J. W. Mintmire, *Phys. Rev. B* **47**, 5485 (1993).
- ⁶R. Saito, G. Dresselhaus, and M. S. Dresselhaus, *Physical Properties of Carbon Nanotubes* (Imperial College Press, London, 1998).
- ⁷M. Bockrath, D. H. Cobden, P. L. McEuen, N. G. Chopra, A. Zettl, A. Thess, and R. E. Smalley, *Science* **275**, 1922 (1997).
- ⁸K. Tsukagoshi, B. W. Alphenaar, and H. Ago, *Nature (London)* **401**, 572 (1999).
- ⁹R. D. Antonov and A. T. Johnson, *Phys. Rev. Lett.* **83**, 3274 (1999).
- ¹⁰Z. Yao, H. W. C. Postma, L. Balents, and C. Dekker, *Nature (London)* **402**, 273 (1999).
- ¹¹R. E. Tuzun, D. W. Noid, and B. G. Sumpter, *Nanotechnology* **6**, 64 (1995).
- ¹²D. Srivastava, *Nanotechnology* **8**, 186 (1997).
- ¹³J. Cumings and A. Zettl, *Science* **289**, 602 (2000).
- ¹⁴S. Berber, Y. K. Kwon, and D. Tománek, *Phys. Rev. Lett.* **91**, 165503 (2003).
- ¹⁵Q. Zheng and Q. Jiang, *Phys. Rev. Lett.* **88**, 045503 (2002); Q. Zheng, J. Z. Liu, and Q. Jiang, *Phys. Rev. B* **65**, 245409 (2002).
- ¹⁶Y. Zhao, C. C. Ma, G. H. Chen, and Q. Jiang, *Phys. Rev. Lett.* **91**, 175504 (2003); C. C. Ma, Y. Zhao, C. Y. Yam, G. H. Chen, and Q. Jiang, *Nanotechnology* **16**, 1253 (2005).
- ¹⁷S. B. Legoas, V. R. Coluci, S. F. Braga, P. Z. Coura, S. O. Dantas, and D. S. Galvao, *Phys. Rev. Lett.* **90**, 055504 (2003).
- ¹⁸J. L. Rivera, C. McCabe, and P. T. Cummings, *Nano Lett.* **3**, 1001 (2003).
- ¹⁹W. L. Guo, Y. F. Guo, H. J. Gao, Q. S. Zheng, and W. Y. Zhong, *Phys. Rev. Lett.* **91**, 125501 (2003).
- ²⁰S. Sapmaz, Y. M. Blanter, L. Gurevich, and H. S. J. van der Zant, *Phys. Rev. B* **67**, 235414 (2003).
- ²¹Y. Zhao, C.-C. Ma, L.-H. Wong, G. H. Chen, Z. P. Xu, Q. S. Zheng, Q. Jiang, and A. T. Chwang, *Nanotechnology* **17**, 1032 (2006).
- ²²M. F. Yu, B. I. Yakobson, and R. S. Ruoff, *J. Phys. Chem. B* **104**, 8764 (2000).
- ²³W. L. Guo, W. Y. Zhong, Y. T. Dai, and S. N. Li, *Phys. Rev. B* **72**, 075409 (2005).